Citation: Liatsis, P., Nazarboland, M. A., Goulermas, J. Y., Zeng, X. J. & Milonidis, E. (2008). Automating the processing of cDNA microarray images. International Journal of Intelligent Systems Technologies and Applications, 5(1-2), pp. 115-144. doi: 10.1504/ijista.2008.018170

Automating the processing of cDNA microarray images

P. Liatsis[1], M.A. Nazarboland[2], J.Y. Goulermas[3], X.J. Zeng[4] and E. Milonidis[1]

[1] School of Engineering and Mathematical Sciences, City University, London, UK

[2] Department of Textiles and Paper, University of Manchester, Manchester, UK

[3] Department of Electrical Engineering and Electronics, University of Liverpool, Liverpool, UK

[4] School of Informatics, University of Manchester, Manchester, UK

Abstract

This work is concerned with the development of an automatic image processing tool for DNA microarray images. This paper proposes, implements and tests a new tool for cDNA image analysis. The DNAs are imaged as thousands of circularly shaped objects (spots) on the microarray image and the purpose of this tool is to correctly address their location, segment the pixels belonging to spots and extract quality features of each spot. Techniques used for the addressing, segmentation and feature extraction of spots are described in detail. The results obtained with the proposed tool are systematically compared with conventional cDNA microarray analysis software tools.

Keywords: cDNA microarrays, gene expression levels, spot detection, addressing, segmentation, feature extraction.

1 Introduction

Over the last decade, scientists have been working toward a complete DNA sequencing of the human genome. Consequently, the focus of genomic research is turning towards looking at how to derive functional information about the newly discovered genes from the vast amount of sequencing information that has been compiled. The analysis of global gene expression patterns is an important new area of genomic research because the development and differentiation of a cell or organism as well as its progression to the disease state is determined largely by its profile of gene expression.

DNA microarrays, in which thousands of different DNA sequences are arrayed in a defined matrix on a glass or silicon support, are part of a new class of biotechnologies, which allow the monitoring of expression levels for thousands of genes simultaneously. By comparing gene expression in normal and abnormal cells, microarrays may be used to identify genes which are involved in particular diseases and can then be targeted by therapeutic drugs.

A DNA microarray is an orderly arrangement of DNA samples. It provides a medium for matching known and unknown DNA samples based on base-pairing rules and automating the process of identifying the unknowns. The first step in the fabrication of microarrays is choosing the cell population. Cells from two different tissues are specialised for performing different functions in an organism. Comparative experiments can reveal genes that are preferentially expressed in specific tissues. Some of these genes implement the behaviours that distinguish the cell's tissue type, while others ensure that the cell only performs the functions for its type. To differentiate between these types of genes, the DNAs are labelled with a reporter molecule that identifies their presence. The end product (microarray) is then scanned and imaged for further interpretation and analysis.

A key step in experiments using DNA microarrays is locating the thousands of individual spots in a scanned array image. Each spot provides quantitative information about a distinct DNA sequence, so it is vital that spots are found and quantified accurately. Spot finding is complicated by variations in the positions and sizes of spots and by the presence of artifacts and background noise in microarray images.

Image analysis is an important aspect of microarray experiments, potentially having a large impact on downstream analysis such as clustering or identification of differentially expressed genes. In a microarray experiment, the arrays are imaged to measure the red and green fluorescence intensities on each spot on the glass slide. These fluorescence intensities correspond to the level of hybridisation of the two samples to the DNA sequences spotted on the slide. These intensities are stored digitally and using image analysis techniques, the data is analysed.

Typically, this task requires carrying out spot detection and segmentation of the pixels corresponding to each individual spot, and feature extraction in terms of intensity estimation and other image quality features. However, the major sources of uncertainty in spot finding are discrete image artefacts, variable spot size and position, and variation of the image background. Image filtering operations are then used to smooth out noise, while robust shape detection algorithms allow feature extraction for each spot.

The spot-finding algorithm is applied to both images (red and green channel) and the features of the corresponding spots are compared to analyse the result of the biological experiment. Similar features in both images indicate a reaction between the two DNAs, whereas spot detection only in one channel is indicative that no such reaction has occurred.

This research describes the development of a fully automated image processing tool for analysis of microarray images. The tool developed can process and analyse as many images as needed without human supervision or intervention. Section 2 provides a literature survey of the currently available microarray image analysis software. Section 3 discusses the type of microarray image data used in this work, while section 4 gives an overview of the proposed microarray image analysis system. The techniques used for gridding, spot segmentation and feature extraction are described in detail in sections 5 through 7. Section 8 provides a comparison of the results of the proposed tool with some of the leading software currently available. Finally, section 9 summarizes the work carried out in this research and provides recommendations for further development of the tool.

2 Overview of existing Microarray Image Analysis techniques

This section reviews the available literature and software tools proposed by academia and industry for the processing of microarrays, with emphasis on image analysis and the fundamental problem of spot finding.

We will firstly present the main steps in microarray image analysis. The first step is *addressing* or *gridding* and is the process of assigning coordinates to each of the spots. The second step is *segmentation* of the desired spots and finally, the third step is *feature extraction* of the corresponding spots.

Gridding

Most software such as Dapple (Zhou et al., 2001), ImaGene (Groch et al., 1999), ScanAlyze (Eisen 1999), GenePix (Axon Instruments, 2002), QuantArray (GSI Lumonics, 1999), Spot (Yang et al., 2000) and an algorithm suggested by (Kim et al., 2001), use the geometry of a microarray, namely, the number and relative spacing of grids, in addition to the arrangement and spacing of spots within each grid, to divide a microarray image into vignettes which contain individual spots. Some of these require manual intervention in order to place the predefined grid over each meta-array. Others insert the predefined grid on the image and it is the user who should adjust the grid over the meta-arrays. The main advantage of this approach is the speed of addressing and locating the grid. However, there are numerous disadvantages with the greatest being user-intervention itself. It is important to automate the entire procedure of image processing to minimise errors due to human intervention, as well as alleviate human operators from such tedious and time-consuming tasks.

Another method called GLEAMS (Zhou et al., 2001) looks for peaks in the 2D periodogram of the image and the distance between the strongest peaks determines the size of the sub-array. A template of a sub-array is then made using the latter and the number of rows/columns. This is used to determine regions in the image that resemble the template. The procedure involves significant pre-processing in terms of image smoothing and noise removal, which is described in detail in (Zhou et al., 2001). The technique is automated and does not require user intervention, however it is time consuming due to computational complexity. Another approach that claims automatic gridding is implemented in AutoGene (Kuklin 2000), however no results are shown or implementation details discussed.

Segmentation

Segmentation of an image can generally be defined as the process of partitioning the image into different regions, each having certain properties (Soille 1999). In the case of microarray image analysis, it is a step to classify the pixels in the image as either being the desired spots (foreground) or the background to the image. The pixels composing the spots are then examined closely to calculate the fluorescence intensities of those particular spots. There exist four groups of segmentation methods, which are explained here. The first method is *fixed circle segmentation*. This method is quite easy to implement and works by fitting a circle with constant diameter to all the spots in the image. However, the main disadvantage of this method is that the spots on the microarray image need to be circular and of the same constant diameter size. ScanAlyze (Eisen 1999) is an example of software using this method. *Adaptive circle segmentation* is the second category, where the circle's diameter is estimated separately for each spot. Two image analysis systems that employ this method are GenePix (Axon Instruments, 2002) and Dapple (Buhler et al., 2000). The advantage of this method over the last one is the varying diameter size, which can correspond to the varying sizes of spots. One of the main disadvantages, however, is the fact that some or most spots are not perfectly circular and can exhibit oval shapes (Eisen and Brown, 1999). As it is important to have no restriction on the shape of the spots, the third category uses *adaptive shape segmentation*. The two most commonly used techniques in this category are the watershed transform (Beucher and Meyer, 1993), (Vincent and Soille, 1991) and seeded region growing (SRG) (Adams and Bischof, 1994). Both these procedures require a starting position (seeds) for the commencement of the segmentation process. There are obvious issues with the use of this method, namely the number of seeds and the selection of seed positions. AutoGene (Kuklin, 2000), ImaGene (BioDiscover, 2001), (Groch et al., 1999) and Spot (Yang et al., 2000) make use of this approach. Another category of segmentation methods used is histogram segmentation employed in GLEAMS (Zhou et al., 2001) and QuantArray (GSI Lumonics, 1999). This class of techniques uses a target mask, which is chosen to be larger than all spots on the image. The histogram of pixel values for pixels inside the masked area approximates the background and foreground intensities for each spot. This method is quite easy to implement but its main disadvantage is that quantification is unstable when a large target mask is set to compensate for spot size variation (Yang et al., 2000). (Nagarajan and Upreti, 2006) use correlation statistics, (Pearson correlation and Spearman rank correlation) to segment the foreground and background intensity of microarray spots. It is shown that correlation-based segmentation is useful in flagging poorly hybridized spots, thus minimizing false-positives. A probabilistic approach to simultaneous image segmentation and intensity estimation for cDNA microarray experiments is followed in (Gottardo and Besag et. al., 2006). In this work, segmentation is achieved using a flexible Markov random field approach, while parameter estimation is tackled using two approaches, namely expectation-maximization and the iterated conditional modes algorithms, and a fully Bayesian framework. A similar modelling framework based on Markov random fields is followed in (Demirkaya and Asyali et. al., 2005). (Lukac and

Plataniotis, 2006) suggest the use of nonlinear, generalized selection vector filters within a vector processing based framework which classifies the cDNA image data as either microarray spots or image background. (Baek and Son et al., 2007) proposed a new approach to simultaneous cDNA image segmentation and intensity estimation by adopting a two-component mixture model. One component of this mixture corresponds to the distribution of the background intensity, while the other corresponds to the distribution of the foreground intensity.

Feature Extraction

The final stage of this process is to calculate the foreground and background intensities of the spots and some measures of spot quality. In almost all microarray image analysis software packages, the foreground intensity is measured as the mean or median of pixel intensity values of the pixels corresponding to the spot.

(Figure 1 near here)

Figure 1 shows the regions considered by different software packages for the calculation of the background intensity for each spot. QuantArray uses the area between two concentric circles (the green circles, which creates a problem when the two spots are very close to each other. ScanAlyze considers all the pixels that are not within the spot mask but are inside a square centred at the spot centre (blue lined square), however this could include some foreground pixels from neighbouring spots. One method that safely deals the above problems is the method used in Spot, which uses four diamond (pink dashed lines) shaped areas between the spots to calculate the local background. (Hua and Liu et. al., 2004) propose microarray BASICA, an integrated image processing tool for background adjustment, segmentation, image compression, and analysis of cDNA microarray images. BASICA uses a fast Mann-Whitney test-based algorithm to segment cDNA microarray images and performs postprocessing to eliminate the segmentation irregularities. The segmentation results, along with the foreground and background intensities obtained with the background adjustment, are then used for independent compression of the foreground and background. A new distortion measurement for cDNA microarray image compression is introduced and a coding scheme is devised by modifying the embedded block coding with optimized truncation (EBCOT) algorithm to achieve optimal rate-distortion performance in lossy coding while still maintaining outstanding lossless compression performance. Further information regarding feature extraction techniques, is given in an excellent reviews by (Petrov and Shams, 2004) and (Rahnenfuhrer, 2005).

3 Experimental Data

The images used in this work are part of a microarray image of *Streptomyces coelicolor*, which belongs to a family of bacteria known as *Streptomycetes. Streptomycetes* are used to produce the majority of antibiotics applied in human and veterinary medicine and agriculture, as well as anti-parasitic agents, herbicides, pharmacologically active metabolites and several enzymes important in the food and other industries.

The microarrays for *S. coelicolor* are produced for global analysis of transcription in Streptomyces. The arrays are used to investigate changes in gene expression during developmental transitions. Streptomyces coelicolor A3(2) has become the paradigm for molecular studies in this group of organisms (Flett et al., 1999) and its study was carried out to analyse global patterns of gene expression and protein synthesis. The sequencing of the 8Mb G+C-rich genome is now almost completed and it is predicted to contain about 7,400 genes. Figure 2 shows an image of a microarray, which corresponds to the expression of *Streptomyces coelicolor*.

(Figure 2 near here)

The microarray is expressed in 4×4 blocks (meta-arrays) and each block has 21×21 spots, hence a total of more than 7000 spots. It is important to note here that each microarray is considered in both green and red channel frequencies. The image in Figure 2 shows the data in grey-scale, however this image can be synthetically coloured red or green corresponding to the dye that the DNAs have been tagged with. In the following sections, only a portion of this image will be shown for testing purposes.

4 Structure of the Image Analysis System

As already mentioned in Section 2, there are three distinct tasks that need to be tackled during the image analysis of microarray images which are as follows:

1- *Addressing*, i.e., the process of assigning coordinates to each spot. The outcome of this stage of the system is to superimpose a grid on the image, hence it is also known as *gridding*.

2- *Segmentation*, which should correctly find the spots of interest on the image and categorically find the pixels that form part of the spot (foreground) or the background.

3- *Feature extraction*, which includes calculating certain statistical intensity features (e.g., mean, median, mode) for each spot and its background. Each pixel in the image has a fluorescent intensity corresponding to the level of hybridisation at a specific location on the slide.

The purpose of microarray image analysis is to find these statistical features, which are subsequently processed by statisticians and biologists, who use mathematical modelling and simulation of these features along with specific biological information obtained from databases to understand gene expression. This makes the final step quite important since statisticians process each spot as a single value (due to large processing time and high storage space needed), which is the combination of all the pixels producing the spot. Of course, in real terms, each spot is made up of between 50-200 pixels. Hence, it is quite important that in the first instance, the spot is fully segmented and secondly the intensities of the pixels making up the spot contribute towards calculating the statistical features of interest.

Estimation of the background intensity is generally considered necessary for the purpose of performing background correction. The reason underlying this is that a spot's measured fluorescence intensity includes a contribution, which is not specifically due to the hybridisation of the mRNA samples to the spotted DNA (Yang et al., 2000). Microarrays are afflicted with discrete image artifacts such as highly fluorescent dust particles, unattached dye, salt deposits from evaporated solvents, and fibres or other airborne debris.

(Figure 3 near here)

Figure 3 is a top-level breakdown of the system structure of the proposed tool for the analysis of microarray images. The following sections concentrate fully on each of the three tasks, describing the techniques used for their implementation and their test results.

5 Addressing

Addressing is an important step in the analysis of the microarray image. Even though it is always best to take into consideration the highest level of accuracy in developing an algorithm, in the case of addressing, it is only necessary to find the approximate location of each spot. Most algorithms and software developed for this purpose require some level of user interaction. However, since the quality of most microarray images is not perfect and there is a requirement for a fully automated system, a novel approach has been proposed here and tested with positive results. In this technique, the image is enhanced, binarised, circular shapes preserved and a statistical method is used to detect the location of each vignette. Figure 4 shows the overall steps undertaken to achieve automatic addressing in microarray image analysis. The following sub-sections fully explain these steps along with the results of testing the corresponding algorithms.

(Figure 4 near here)

5.1 Thresholding

The addressing algorithm uses morphological operators to preserve shapes and the binary version of the image to locate each vignette. For this reason, the image is first binarised and hence the first operation applied to the image is thresholding. Otsu's thresholding algorithm (Otsu 1979) is the first technique that was tested with microarray images. The algorithm determines a threshold value, which maximises a measure of the separability of the two classes, i.e., background and foreground. Otsu's method was unable to find most of the spots in the image since there is a large number of noise artefacts in the image. One way of tackling this problem is to require the user to intervene by selecting the location of blocks of spots using the mouse (interactive thresholding). However, this compromises the objective of automated analysis of the tool and hence was not explored further.

In the case of addressing, thresholding is used to extract the spots from the background. It is not quite imperative to segment all the pixels that form the spot since the addressing of the spots provides just an estimate of their position; however, the majority of the pixels contributing to each spot should be found. Following careful consideration and systematic application of diverse thresholding values to various microarray images, a method of threshold selection has been chosen. The threshold value was found empirically to be at about 1% of the maximum grey-level value (i.e., 600).

(Figure 5 near here)

Figure 5 shows the effect of thresholding with different threshold values. It can be seen from these images that the threshold value of 600 provides satisfactory results. Lower threshold values classify parts of the background (see Figure 5(a) and (b)) as belonging to the foreground; in this case, the majority of the image is classified as belonging to the spots (and marked as “white”). Higher threshold values do not detect all spots or the majority of their pixels (as is the case in Figure 5(d)).

5.2 Image Smoothing

In order to tackle noise originating, for instance, from dust, which can sometimes be detected, a variety of linear and non-linear filtering techniques were applied, however their performance was not deemed satisfactory. Instead it was decided to attempt the use of morphological operators as a means of removing noise, while preserving the circular shape of the spots. Morphological operators are used predominantly for noise filtering, shape simplification, enhancing object structure and of course segmenting objects from background.

We apply the opening transformation (Schalkoff 1989), which is generally used to preserve specific shapes in the image and a structuring element of a defined shape is used to preserve the corresponding shape. Opening can be used in the first instance to remove noise from the image and secondly as an operation to preserve circular shapes in the image. There are two types of noise in the image that can complicate further processing. There are some noise patterns, which typically have a size less than the smallest spot size, and some which are considerably larger. The former type of noise can be removed when the filter for preserving the spots is applied, however, the latter type needs to be targeted first. It is known that the spot diameters are typically between 8-16 pixels. Hence, an 18×18 square filter is applied to the image, which preserves any shape that corresponds to a large square. This filter obviously targets and preserves any object on the image larger than the biggest spot.

(Figure 6 near here)

Figure 6 shows how the first type of noise is removed. First, all objects larger than the spots are preserved (using the opening operator), and then the preserved objects are removed from the original image to leave an image that does not contain this noise. The above images are the top part of the image in Figure 2, which does not contain any useful information (no DNA representation) and is made up of noise only. Not only is this mask larger than the spot, but it is also square shaped since the spots are of circular shape. This will satisfy the requirement that the spots should not be preserved. Next, a circularly shaped mask is used to preserve the spots since most spots are circular. It has a diameter of nine pixels, which corresponds to the smallest possible spot radius. It is important to note that the current pixel where the mask is positioned is at the centre of the mask. As it is needed to preserve all the spots on the image, the smallest spot (with diameter of nine) is considered so that all spots are preserved. Figure 7 shows the result of noise removal and preservation of circularly shaped objects.

(Figure 7 near here)

5.3 Grid Placement

This subsection describes the approach followed for grid placement in microarray images. The algorithm is based on the extraction of 1D signatures in the horizontal/vertical directions. The proposed techniques make use of the proximity of spot objects. Hence, by evaluating the 1D signatures of the DNA image, we can ascertain whether there is an accumulation of foreground pixels, which would then indicate the presence of a block of spots. The procedure of 1D signature extraction is applied to each row/column of the image, by simply counting the number of foreground pixels. The primary means of detecting the boundaries was through the first- and second-order derivatives of the intensity signal (Schalkoff 1989). The zero-crossings of the first-order derivatives indicate the position of the peaks and valleys in the signal, whereas the sign of the second-order derivative in these locations can specify whether that point is a peak or a valley in the signal. However, prior to differentiating, the signal should be smoothed with a Gaussian filter to remove false peaks/valleys within another peak. These false peaks/valleys arise due to spots not being aligned perfectly in one horizontal/vertical line (row/column).

(Figure 8 near here)

Figure 8 shows the 1D signal, its first and second-order derivatives, where the zero crossings of the first-order difference signal indicate the location of the peaks and valleys in the signal. These are very useful points since they can indicate the location of the spot/meta-array boundaries. However, these peaks and valleys are present in the noisy section of the signal, thus, further processing is needed to locate the true valleys. In order to eliminate the peaks/valleys corresponding to the noisy sections of the signal and to choose the correct valleys to designate the location of the spot/meta-array boundaries, we make use of the procedure of hierarchical clustering.

A hierarchical clustering algorithm (Arabie et al., 1996) constructs a tree of nested clusters based on proximity information. The primary purpose for building a cluster hierarchy is to structure and present data at different levels of abstraction. The first step in performing hierarchical clustering analysis on a data set is to find similarity or dissimilarity between every pair of objects in the data set by calculating the Euclidean distance between them. The next stage is to group the objects into a binary, hierarchical cluster tree. In this step, pairs of objects that are in close proximity are linked using the “shortest distance” information generated in the last step. As objects are paired into binary clusters, the newly formed clusters are grouped into larger clusters until a hierarchical tree is formed. Finally, the objects in the hierarchical tree are divided into clusters by detecting natural groupings in the hierarchical tree or by cutting off the hierarchical tree at an arbitrary point.

The data set input to the hierarchical clustering algorithm is the distance of the peak points from the beginning of the signal (i.e., column number). Hierarchical clustering is therefore used to determine the closest points. Based on this data set, the *shortest distance* method of cluster tree construction is used. The basis of linking data points in this method is grouping points closest to one another. Figure 9 shows the resulting tree structure, indicating five distinct clusters, using the shortest distance linking method.

(Figure 9 near here)

(Figure 10 near here)

By examining the number of elements in each group of clusters, it can be deducted that one cluster is associated with noise and the other four are the true peak points, belonging to the four meta-arrays. Figure 10 shows the final outcome of the clustering algorithm indicating which peak points belong to which cluster (meta-array).

(Figure 11 near here)

However, the location of peak points does not imply the location of the spot/meta-array boundaries. These are indicated by the valleys in either side of each peak point. The first and last member of each cluster imply the locations of the meta-array boundaries, while the ones within each cluster imply the locations of spot boundaries. The Gaussian smoothing applied to the original data ensures that the valleys prior and subsequent to each peak point inside each cluster are the true valleys, by removing the false peaks/valleys at the early stages. Figure 11 shows the final result of superimposing the non-uniform grid on the microarray image.

5.4 Locating individual spots

There are two means of finding the exact co-ordinates of each spot; either with the technique used to find meta-array locations or by simply examining each position and if the pixels that follow it have intensities in an ascending/descending order, it is the starting/ending position of the spots in that row/column.

(Figure 12 near here)

The discontinuities in the data are taken as a probable location for a spot, however these discontinuities could correspond to noise in the meta-array. For this reason, for every discontinuity, the neighbouring values are examined and if the intensities of the pixels preceding it are on the decrease while the ones following it are on the increase, the current location is the starting/ending position of the spot. After using the horizontal/vertical 1-D signatures of the image to find the coordinates of each meta-array, and the horizontal/vertical 1-D signatures of each meta-array to find the coordinates of spot vignettes, the algorithm is able to superimpose a non-uniform grid over the image. Figure 12 shows the result of superimposing the non-uniform grid on the image. Determining the approximate positions of the spots was the first part of the algorithm. The main part is to locate the pixels that construct a spot, so that their fluorescent intensities are extracted. Segmentation is used to locate these pixels.

6 Spot Segmentation

Segmentation is the process of decomposing images into separate regions such that particular features can be extracted from them. A combination of edge detection and region analysis techniques were used for spot segmentation in the proposed system. Edge detection is the detection of significant changes in some physical aspect of the image and is evident in the image as changes in intensity, colour and texture. Since in the current approach, edge detection is used in conjunction with region analysis (edge detection is used to find the pixels belonging to the spot boundary, followed by region analysis to extract all the pixels inside each spot), thus it is important that the resulting edges are connected together. Two edge detection techniques that were successfully applied are the Canny and Laplacian of Gaussian (LoG).

(Figure 13 near here)

Figure 13 shows the steps in the spot segmentation algorithm. It shows that both Canny and LoG edge detection techniques are used, the former using its output as an input to the circle detection algorithm to verify and choose spots which are circular, whereas, the latter uses its output as the boundary (edges) for every spot. Starting with a seed corresponding to the centre of the circle and this boundary, using a flood-filling algorithm, all the pixels belonging to a spot are segmented and are ready for information extraction.

6.1 Canny Edge Detection

Canny proposed an optimal approach to edge detection (Canny 1983), (Canny, 1986), based on three criteria. Firstly, it is important that edges occurring in images should not be missed and that there are no responses to non-edges (low error rate). Next, edge points are well localized, i.e., the distance between the edge pixels found by the edge detector and the actual edge is minimised. Finally, there is only one response to a single edge. Based on these criteria, the Canny edge detector first smoothes the image to eliminate noise. It then finds the image gradient to highlight regions with high spatial derivatives. The algorithm then tracks along these regions and suppresses any pixel that is not an edge (non-maximum suppression). The gradient array is now further reduced by hysteresis. Hysteresis is used to track along the remaining pixels that have not been suppressed. Hysteresis uses two thresholds, if the magnitude is below the first threshold, it is set to zero (set as a non-edge point). If the magnitude is above the high threshold, it is labelled as an edge point, and if the magnitude is between the two thresholds, then it is set to zero unless there is a path from this pixel to a pixel with a gradient above the high threshold.

There are three parameters that need to be selected when using the Canny edge detector; these are the sigma value, which determines the size of the Gaussian filter and the upper and lower thresholds in the hysteresis stage. Extensive testing was carried out to test for different values of these parameters. The results showed that the optimal values are a standard deviation of 2.7, an upper threshold of 65% and a lower threshold of 25% of the maximum grey value (i.e., 42598 and 16384, respectively with the maximum grey level of 16 bits or 65535).

6.2 The Gerig Hough Transform

The Hough Transform (HT) is a method of detecting complex patterns of points, described by analytical equations in image data (Hough, 1962). The HT requires that the edge elements are first enhanced/detected and then the edge map image is thresholded. The extracted edge pixels are then processed to accumulate a set of votes, which designates probabilities for a number of solution categories. The HT can be seen as an evidence gathering procedure (Illingworth and Kittler, 1988). Particularly, each edge primitive votes for all parameters that could have produced it, if it was part of the required shape. After the final votes are collected, the highest ones are indicative of the relative likelihood of shapes defined by the parameters corresponding to those votes.

One of the problems with the standard Hough Transform is the large storage space required when the range of circle radii is large. Gerig (Gerig and Klein, 1986) proposed a technique by reordering the HT calculation to replace the 3D accumulator of size N^3 by three 2D arrays of size N^2. The Gerig Hough transform (GHT) performs the full HT as a series of HTs in which, at each stage, there is only a single value of radius to guide the transform. At each stage, a 2D array acts as working space (C_W) for transform accumulation and local peak finding. Peaks are characterised by their position, their size and the radius for which the transform is accumulated which can be recorded in the appropriate bins of two 2D arrays (C_P, C_R) matching the working array. At each stage, the working array is initialised and used to calculate the transform for another value of radius r. This process is repeated for all possible distinct radii. At the end of the process, the two 2D arrays contain information about location, size and radius of transform peaks. We make use of the Gerig HT with Gradient information (GHTG). This has low memory requirements, since the three accumulators (in an m×n image) require 3×m×n cells in total, hence giving a space complexity of O(m×n) at the expense of inability to locate concentric circles; a 3D cubic a-b-r accumulator is unnecessary.

Every feature point P casts one vote in C_W which in the standard implementation is set to one. In order to make the accumulated evidence more objective, every point P generates a vote V(P) which depends on its gradient magnitude G(P). This is an adaptive incrementation scheme and enables strong edge points to outweigh other noisy ones which usually have lower edge magnitudes, resulting in a reduction of noise in parameter space. V(P) is bounded by a maximum and a minimum value to avoid unreasonable vote values. In addition, to prevent weaker edges from being completely masked off by stronger ones, an exponential voting system can be used (Goulermas et al., 1995). Interpreting the transform space is the final task of the HT. After the total transform has been accumulated, C_P and C_R contain information about the centres and the radii of the circles. Hence, the next step involves analysing the accumulated votes, so that true peaks that indicate the parameters of actual shape instances are objectively detected.

(Figure 14 near here)

The simplest method of peak detection (Ballard and Brown, 1982) is the global thresholding of the accumulator. A predefined threshold can differentiate between peak and non-peak bins. However, problems caused by image discontinuities, inaccuracies in edge orientation, noisy feature points and non-perfectly circular boundaries add noise to C_P, spreading the peak to neighbouring cells and changing its height and position. To address this, accumulator filtering is applied (Goulermas et al., 1995). C_P is sharpened with a high-pass filter, so that the real peaks are accumulated and false ones are downcast. After accumulator filtering which also sharpens the peaks, thresholding is applied to locate the peaks. Figure 14 shows the result of circle detection using the Gerig Hough Transform with gradient information for different peak thresholds.

6.3 Laplacian of Gaussian Edge Detection

Even though Canny edge detection provides a suitable input to the GHTG, it is not sensitive enough to find weaker pixels that contribute to the spots under investigation. Thus, using Canny edge detection does not guarantee that all spots will be accurately segmented. On the other hand, the Laplacian of Gaussians (LoG) is quite sensitive and can detect pixels which could potentially belong to the corresponding spots. This very sensitivity however causes some noise to be detected in the image.

The next step in the development of the tool is to find the variations in parameters in the LoG edge detection method. The only parameter that needs to be defined is the standard deviation of the Gaussian, or simply, the size of the mask to be applied to the image. Small mask size (or small standard deviation) can contribute to less noise removed causing the output result to make the edges of the noise connect to the edges of the spots. A large mask size would not only remove noise but it could also remove some parts of the spots (data) that are very weak. Experimentation with the arrays available and the strength ratio of the noise versus image data led to approximating the standard deviation value and hence the mask size was chosen to be 9×9. The LoG edge detected image along with the circle centres are then used as input to the flood-filling algorithm to extract all the pixels belonging to a spot.

6.4 Flood-Filling Algorithm

The Flood-filling algorithm (Liatsis, 2002) is a seeded region growing segmentation technique. Using the GHTG, circularly shaped spots were detected and also the GHTG was able to find the centre of its proposed circle. The Laplacian of Gaussian determined the edges of these spots and hence the boundary that separated the spot from the background. In the flood-filling algorithm, the circle centre is used as a seed point and this seed can be grown to find all the pixels that compose the spot. This is a recursive algorithm, which operates until all the pixels inside the spot boundary are marked as belong to the spot or the boundary. In the proposed tool, a 4-connected algorithm is used. The reason behind this choice is the shape and thickness of the boundary. The boundary found using the LoG is only one pixel wide and in certain cases, the 8-connected algorithm can move across the boundary and hence count the background pixels as parts of the spot being investigated. The flood-filling algorithm starts from the circle centre coordinates as the seed point and moves to the four neighbours of this pixel, checking for the condition that they lie inside the boundary of the spot. This is done in one direction (one neighbour) at a time. If the pixel being investigated lies inside the boundary, it is flagged and counted as a spot pixel. The reason for flagging it is for a pixel not to be counted more than once. The procedure continues until the algorithm comes to a halt in all directions. This ensures that all the spot pixels are segmented without moving outside the spot boundary set. The pixels are divided into two categories, i.e., edge pixels and spot pixels.

7 Feature extraction

In the microarray experiments, both DNAs are tagged with different probes. A laser excites these probes and they are imaged with a scanning confocal microscope. These images are investigated and if the same spot exists in the same location on the two images, it means that the complementary DNA and the sample DNA have bonded. The whole basis of the tool developed for processing of microarrays is to extract the features of the spots found so that they can be compared and contrasted in the two channels to analyse if the genetic experiments have been successful. One of the most common techniques is to extract the fluorescent intensity for individual spots, however as spots are composed of numerous pixels, comparison can be complicated. For this reason, the mean, median and mode intensities of each spot are calculated and used for comparison. An important issue with the intensity values is that they are proportional to the time after the reaction. Since, two images of the same microarray in different channels (usually red and green) are taken separately, one could have been over-exposed making the comparison difficult. To overcome this, these values need to be normalised. This is done by the system biologists and is not within the scope of this tool.

Alternative methods of comparison were investigated and integrated as part of this tool. One such method exploits the shape parameters of the spots. Spot area, circle centre coordinates and spot compactness were used as benchmarks for comparison.

7.1 Intensity extraction

The proposed tool has successfully located the spots (addressing) and segmented the pixels that contribute to the particular spot (segmentation). This step is done concurrently with the flood-filling algorithm. As spot pixels are detected, their corresponding fluorescent intensity is extracted. The extracted information is stored for further processing.

7.2 Background Extraction

The background surrounding each spot is separated from the rest of the image by the non-uniform grid superimposed at the initial stages of the image processing. After the flood-filling algorithm, any pixels inside the vignette that are not marked as a foreground (spot) pixel are set as background pixels by default.

(Figure 15 near here)

Figure 15 shows the boundaries that contain the pixels making up the background. As it can be seen, red and grey indicate extracted spot and edge pixels, respectively. All the pixels remaining inside the vignette (made up by white lines) are assumed to be part of the background.

7.3 Mean, Median and Mode Intensities

There exist some statistics that characterise the distribution of a random variable. The three most commonly used parameters to define the centre of a distribution are *mean*, *mode* and *median*. The mean is the centre of gravity of the distribution and can be easily found as the sum of all values divided by the number of values. The mode is defined as the elementary event for which the probability density function has the maximum value. This corresponds to the highest possible value in the distribution. And finally, the median is the middle value of the distribution. It is evident that both background and foreground intensities stored earlier can be used to calculate the three different statistical parameters defined. The above procedures are applied to both foreground and background intensities.

7.4 Compactness

Another property of each spot that can be compared is compactness or circularity. This identifies how closely packed the shape is and is defined as perimeter^2/area. The most compact shape in Euclidean space is the circle having a compactness of 4π, hence, if the compactness of each spot is calculated and then divided by 4π, the closer the corresponding value is to one, the more circular the shape is. The perimeter of the shape is the number of pixels found to be the boundary of each spot (using LoG edge detection), while the area is the number of pixels that belong to the spot (found using the flood-filling algorithm). These values are then used to calculate the circularity of each spot, which can be used as a parameter for comparison between the two images.

8 Comparison of Results

The software tool developed in this work is compared with three other tools, namely, TIGR SpotFinder (TIGR SpotFinder, 2001), ScanAlyze (Eisen, 1999) and ImaGene (BioDiversity, 2001). Twenty-five images of *Streptomyces coelicolor* were used for testing. Figure 16 shows a portion of a microarray image used for testing purposes.

(Figure 16 near here)

One of the main differences in alternative software packages and the tool described here is the artificial colouring used in images. This can be easily achieved, however, since the tool developed is fully automatic, it does not require any changes to the image for human inspection. On the other hand, the other techniques rely on the user placing the grid and then the software takes over to start the spot analysis, hence, image colouring is one way of helping the user decide on the location of spots.

The first step of analysis is the determination of a grid and addressing of the spots. This is the main difference between the tools. In the three tools tested, grid placement was the responsibility of the user whereas it is found automatically in the tool developed. In all three tools, the user is asked for the number of meta-arrays and number of rows and columns of spots inside those arrays, the spacing between spots and the spot size (width and length). Using the information input by the user, a grid is formed and it is the user's responsibility to place the grid over the image correctly. Next, the user needs to verify and correct the location of each vignette over a spot. On each image, there could be as many as 8000 spots and possibly more than a few images for each experiment. This is a very time consuming procedure and the user has to be present for supervision of every microarray image analysis experiment. However, in the tool developed here, we can process as many images as necessary for analysis with no user supervision (or intervention). It is important to note that the user has the ability to intervene in the analysis of the image if they want to and this is facilitated in the tool developed.

The next step in processing microarray images after addressing is segmentation. The three tools heavily rely on the addressing (and the grid placed over the image as its result) to apply local segmentation inside each vignette. The ScanAlyze software package goes one step further and uses the grid positions (and shape) as a priori information used for segmentation. The grid placed by the user is of circular shape and is used by the tool to segment the spot.

(Figure 17 near here)

Basically, the tool captures all the pixels inside the circular grid as belonging to a spot. Figure 17 shows the shortcomings of the segmentation method (fixed circle segmentation) used by the ScanAlyze tool. The grid circle could contain some of the background while some of the foreground information may be missing. This leads to an incorrect output result, which can lead to failure in determining the result of the biological experiment.

Figure 18 shows the difference in segmentation between TIGR SpotFinder and the tool developed when comparing the segmentation area in corresponding spots. As it can be seen, the detected spot area is bigger in the latter and also the segmentation of the spot found by the former shows clearly that not all the pixels belonging to the spot are segmented.

(Figure 18 near here)

The main advantage of the segmentation technique used in the tool developed over its peers is the use of a combination of adaptive shape and circle segmentation. In this tool, varying circle size masks are used to locate circular shapes in the image and the corresponding spot is segmented no matter what shape it may possess, hence all of its pixels are segmented. ImaGene uses an adaptive shape segmentation only which leads to some noise to be segmented.

Feature extraction is the most important part of microarray images analysis. Most of these tools use the spot and background statistics (mean, median and mode) along with the number of pixels making up the spot and the background. Some other features are also used, but the basis of all is correct segmentation of the spots. For this reason, as it was discussed above, ScanAlyze and TIGR SpotFinder fail in finding correct results for any of the above statistics since the segmentation is not satisfactory enough to locate all the pixels contributing to the spot and even in some cases some of the background is detected.

Tables 1-4 show a portion of the output result tables from the four tools tested. Special notice should be paid to the spot area. In both ScanAlyze (equal number of pixels in all spots since fixed circle segmentation is used) and TIGR SpotFinder, this area is smaller than the one found by the tool developed here. This can be easily verified with the naked eye (as in Figures 17 and 18) to see that some of the pixels belonging to the spots are not detected, hence, the resulting mean, median and mode intensities are not properly calculated.

Row No	Col No	Mean Spot Intensity	Mean BG Intensity	Median Spot Intensity	Median BG Intensity	Total Intensity	Spot Area	BG Area
1	1	6128	97	6530	86	821239	134	1802
1	2	12306	96	13123	82	1230638	100	1836
1	3	11004	101	12798	87	1199507	109	1827
1	4	7878	103	9256	88	1063610	135	1801
1	5	8236	100	9364	88	938990	114	1822
1	6	9234	98	10263	90	1172762	127	1809
1	7	11365	98	13533	84	1420748	125	1811
1	8	16054	98	17023	84	2038861	127	1809
1	9	18455	103	19764	82	2011674	109	1827
1	10	5572	106	6141	84	752317	135	1713
2	1	16043	101	17324	79	1796927	112	1824
2	2	12236	105	14163	83	1529506	125	1811
2	3	11358	98	12873	84	1226672	108	1828
2	4	2727	92	2981	87	354580	130	1806
2	5	16919	97	18342	88	2081098	123	1813
2	6	3020	94	3973	90	413856	137	1799
2	7	60092	207	64536	97	5588556	93	1893

Table 1: Portion of the output result table obtained from the proposed tool

Row No	Col No	Mean Spot Intensity	Mean BG Intensity	Median BG Intensity	Spot Area	BG Area
1	1	7278	168	85	97	1584
1	2	12654	99	86	97	1584
1	3	12166	114	90	97	1584
1	4	9542	190	86	97	1584
1	5	9203	130	87	97	1584
1	6	11293	144	87	97	1584
1	7	12945	201	85	97	1584
1	8	19181	253	90	97	1584
1	9	19579	217	86	97	1584
1	10	6526	181	89	97	1584
1	1	19442	128	89	97	1584
1	2	14594	177	83	97	1584
1	3	12327	118	85	97	1584
1	4	3350	108	85	97	1584
1	5	21252	150	89	97	1584
1	6	3624	132	86	97	1584
1	7	53080	749	89	97	1584

Table 2: Portion of the output result table obtained from ScanAlyze

Row No	Col No	Mean Spot Intensity	Total Intensity	Spot Area
1	1	7120	733366	103
1	2	12696	1218812	96
1	3	12239	1174976	96
1	4	9402	940232	100
1	5	9034	894348	99
1	6	11290	1095088	97
1	7	13480	1348028	100
1	8	20342	2034173	100
1	9	20825	2040865	98
1	10	6639	657306	99
2	1	1980	221762	112
2	2	8641	872782	101
2	3	3601	334850	93
2	4	3069	322290	105
2	5	2221	228718	103
2	6	4303	421654	98
2	7	7259	566172	78

Table 3: Portion of the output result table obtained from TIGR SpotFinder

However, this area is larger in the output results found by ImaGene. This leads to considering some background pixels belonging to the foreground, hence leading to the corruption of the statistical data. Since, spot segmentation algorithms in ImaGene are not fully described, this tool was tested using its corresponding results.

Testing the different tools we may conclude that firstly, they do not offer a fully automatic software, which can process images without user intervention. Secondly, methods and algorithms used in segmentation of spots do not locate all the pixels belonging to a spot or sometimes include some of the pixels contributing to the background. The latter case can damage the result of the analysis. However, the software tool developed here works automatically, allows user intervention (if necessary) and locates pixels belonging to a spot correctly.

Row No	Col No	Mean Spot Intensity	Mean BG Intensity	Median Spot Intensity	Median BG Intensity	Total Intensity	Spot Area	BG Area
1	1	5554	91	6660	82	833030	150	1875
1	2	11456	94	13129	85	1237280	108	1872
1	3	10229	98	12358	88	1207072	118	1906
1	4	7217	94	8177	82	1082560	150	1875
1	5	7701	96	9155	84	947270	123	1902
1	6	8744	93	10102	85	1180454	135	1845
1	7	10734	97	12373	85	1427673	133	1892
1	8	15749	96	18837	87	2110300	134	1936
1	9	17181	93	19163	83	2096130	122	1902
1	10	5479	97	5964	85	756158	138	1774
2	1	16269	97	18674	88	1935975	119	1861
2	2	10809	91	12989	79	1556502	144	1926
2	3	10662	93	13061	84	1236777	116	1954
2	4	3019	93	3299	83	350180	116	1908
2	5	16090	94	19667	88	2156122	134	1890
2	6	2888	93	3082	84	418811	145	1835
2	7	58832	281	65535	86	5824408	99	1926

Table 4: Portion of the output result table obtained from ImaGene

The features of the spot consist of the mean, median and mode of the intensities of the pixels composing the signal (foreground) and the background, along with the total intensities for the pixels composing the spot and the background are all tabulated in the output result. The spot area and perimeter (which are used to calculate the compactness of the spot) are followed by the circularity value in the output table. Other outputs of this tool are the Canny and LoG edge detected images and also the circle-detected image. There is an option for the non-uniform grid to be positioned over the image, which should be selected prior to the start of the image processing algorithms.

9 Conclusions

This work presented and discussed the methods and algorithms along with test results in the development of a microarray image processing and analysis tool. The tool was developed in the three main stages of addressing, segmentation and feature analysis.

It first proposed an algorithm for automatically locating spots on the image leading to the superimposition of a non-uniform grid over the image. The scheme used morphological opening as both a smoothing operator and also to preserve circularly shaped objects in the image. Next, the system used both adaptive shape and circle segmentation techniques. The fluorescent intensities of these spots were then extracted and these were recorded in a table along with other feature quality analysis parameters such as mean, median and mode intensities, signal and background area and compactness of the shape detected.

Finally, the tool developed was compared against three other tools to determine the advantages/disadvantages of the former over these tools. The most important difference was found to be the fact that the tool developed here is fully automatic, whereas the three tools tested needed user intervention especially in determining and placing a grid over the image. The other main difference was in the techniques used in segmenting spots, where the other tools failed to fully segment all the pixels composing a spot, and in some cases even some of the background was detected as belonging to a spot.

There are various avenues for potential continuation and improvement of the work presented here. There exist some images of reduced quality in terms of the presence of potential spots. In these images apart from noise, some cDNAs are not detected and hence the image provides a poor estimate of spot numbers. On the other hand, the gridding algorithm proposed in this contribution depends on the accumulation of spots in horizontal/vertical lines before detecting them using statistical techniques. Thus, this aspect causes a problem for images with more than half the number of possible spots missing in addressing and locating spots.

Another area of improvement follows spot detection. Currently, the proposed tool only removes background, i.e., noise that is not attached to spots. This needs to be rectified so that noise contributing to spot pixel intensities is eliminated from the final output result. Further analysis of the histogram statistics of each spot would provide a means for suppressing erroneous information.

In spot segmentation, other techniques should be considered. One such technique is seeded region growing (SRG) (Adams and Bischof, 1994). The problem faced in this algorithm is the method of automatic seed selection. Alternatively, pulsed coupled neural networks (PCNN) (Kuntimad and Ranganath, 1999) have been utilised in image segmentation. The general approach to segment images using PCNN is to adjust the parameters of the network so that the neurons corresponding to the pixels of a given region pulse together and the neurons corresponding to the pixels of adjacent regions do not pulse together.

References

R. Adams and L. Bischof, “Seeded region growing,” IEEE Transactions on Pattern Analysis and Machine Intelligence, pp. 641-647, vol. 16, No. 6, 1994.

P. Arabie, L. J. Hubert and G. De Soete, “Clustering and classification”, World Scientific, 1996.

J. Baek, Y.S. Song, G.J. McLachlan, “Segmentation and intensity estimation of microarray images using a gamma-t mixture model”, Bioinformatics, Vol. 23, No. 4, pp. 458-465, 2007.

D. H. Ballard and C. M. Brown, “Computer Vision”, Prentice-Hall, 1982.

S. Beucher and F. Meyer, “The morphological approach to segmentation: the watershed transformation,” Mathematical morphology in image processing, vol. 34 of Optical Engineering, pages 433-481, Marcel Dekker, New York, 1993.

BioDiscovery, Inc., “ImaGene 4.1,” user’s manual, 2001.

J. Buhler, T. Ideker and D. Haynor, “Dapple: Improved techniques for finding spots on DNA microarrays,” UW CSE technical report UWTR, 2000.

J. F. Canny, “Finding edges and lines in images”, Technical Report AI-TR-720, MIT, Artificial Intelligence Laboratory, Cambridge, MA, 1983.

J. F. Canny, “A computational approach to edge detection”, IEEE Transactions on Pattern Analysis and Machine Intelligence, pp. 679-698, vol. 8, 1986.

I. J. Cox, S. L. Hingorani and S. B. Rao, “A maximum likelihood stereo algorithm”, Computer Vision and Image Understanding, pp. 542-567, Vol. 63, No. 3, May 1996.

M. B. Eisen, “ScanAlyse documentation,” 1999.

O. Demirkaya, M.H. Asyali, M.M. Shoukri, “Segmentation of cDNA microarry spots using Markov random field modelling”, Bioinformatics, Vol. 21, No. 13, pp. 2994-3000, 2005.

M. B. Eisen and P. O. Brown, “DNA arrays or analysis of gene expression”, Methods in Enzymology, 303, 1999.

F. Flett, D. Jungmann-Campello, V. Mersinias, S.L.-M. Koh, R. Godden, and C.P. Smith, "A ‘Gram-negative-type’ DNA polymerase III is essential for replication of the linear chromosome of Streptomyces coelicolor A3(2)" Mol Microbiol, pp. 949-958, vol. 31, 1999.

G. Gerig and F. Klein, “Fast contour identification through efficient Hough Transform and simplified interpretation strategy”, 8th International Joint Conference on Pattern Recognition, Paris, pp. 498-500, 1986.

R. Gottardo, J. Besag, M. Stephens and A. Murua, “Probabilistic segmentation and intensity estimation for microarray images”, Biostatistics, Vol. 7, No. 1, pp. 85-99, 2006.

J. Y. Goulermas, P. Liatsis and M. Johnson, “Real-time intelligent vision systems for process control”, Proceeding of 4th IchemE Conference on Advances in Process Control, York, pp. 69-76, 1995.

K. Groch, A. Kuklin, A. Petrov and S. Shams, “Image segmentation and quality control measures in microarray image analysis”, JALA, vol. 6, no. 3, July 2001.

GSI Lumonics, “QuantArray analysis software,” Operator’s Manual, 1999.

P. V. C. Hough, “Methods and means for recognising complex patterns”, US Patent 3069654, 1962.

J.P. Hua, Z.M. Liu, Z.X. Xiong, Q. Wu and K.R. Castleman, “Microarray BASICA: Background adjustment, segmentation, image compression and analysis of microarry images”, EURASIP J Applied Signal Processing, Vol. 1, pp. 92-107, 2004.

J. Illingworth and J. Kittler, “A survey of the Hough Transform”, Computer Vision Graphics and Image Processing, pp. 87-116, vol. 44, 1988.

J. H. Kim, H. Y. Kim and Y. S. Lee, “A novel method using edge detection for signal extraction from cDNA microarray image analysis”, Experimental and Molecular Medicine, pp. 83-88, vol. 33, no. 2, 2001.

A. Kuklin, “Automation in microarray image analysis with AutoGene”, JALA, vol. 5, Nov. 2000.

G. Kuntimad and H. S. Ranganath, “Perfect image segmentation using pulsed coupled neural networks”, IEEE Transactions on Neural Networks, Vol. 10, No. 3, May 1999.

P. Liatsis, “Intelligent visual inspection of manufacturing components”, Ph.D. Thesis, UMIST, UK, 2002.

R. Lukac and K.N. Plataniotis, “cDNA microarray image segmentation using root signals”, Int J Imaging Systems and Technology, Vol. 16, No. 2, pp. 51-64, 2006.

R. Nagarajan and M. Upreti, “Correlation statistics for cDNA microarray image analysis”, IEEE-ACM Trans. Computational Biology and Bioinformatics, Vol. 3, No. 3, pp. 232-238, 2006.

N. Otsu, “A threshold selection method from grey-level histograms”, IEEE Trans. Systems, Man and Cybernetics, pp. 62-66, vol. 9, 1979.

A. Petrov and S. Shams, “Microarry image processing and quality control”, J VLSI Signal Processing Systems for Signal, Image and Video Technology, Vol. 38, No. 3, pp. 211-226, 2004.

J. Rahnenfuhrer, “Image analysis for cDNA microarrays”, Methods of Information in Medicine, Vol. 44, No. 3, pp. 405-407, 2005.

J. Schalkoff, “Digital Image Processing and Computer Vision”, J. Wiley and Sons, 1989.

P. Soille, “Morphological Image Analysis: Principles and Applications”, Springer, 1999.

TIGR SpotFinder, “http://www.tigr.org/software/tm4/”, for software and documentation, 2001.

L. Vincent and P. Soille, “Watersheds in digital spaces: An efficient algorithm based on immersion simulations”, IEEE Transactions on Pattern Analysis and Machine Intelligence, pp. 583-598, vol. 13, 1991.

P. E. Wellstead and M. B. Zarrop, “Self tuning systems: control and signal processing”, Wiley, 1991.

Y. H. Yang, M. J. Buckley, S. Dudoit and T. P. Speed, “Comparison methods for image analysis on cDNA microarray data”, Technical report # 584, Nov. 2000.

Z. Z. Zhou, J. A. Stein and Q. Z. Ji, “GLEAMS: A novel approach to high throughput genetic micro-array image capture and analysis”, Proceedings of SPIE vol. 4266, 2001.

Axon Instruments, Inc., “GenePix Pro 4.1,” user’s guide and tutorial, 2002.

Biographical notes

Dr Panos Liatsis is a Senior Lecturer and the Director of the Information and Biomedical Engineering Centre at City University, London. He obtained his first degree in Electrical Engineering from the University of Thrace and his PhD from the Control Systems Centre, Department of Electrical Engineering and Electronics at UMIST. His research interests are in the areas of pattern recognition, image analysis and intelligent systems, with applications to biomedical engineering. He has published over 100 papers in the proceedings of international conferences and high-impact factor international journals. He is a member of the IEE, the IMC and the IEEE.

Mr Mohammed Ali Nazarboland is a PhD student in the Department of Textiles and Paper in the University of Manchester. He obtained his first degree in Computer Systems Engineering and his MPhil from the Control Systems Centre, Department of Electrical Engineering and Electronics, at UMIST. His research interests are in the areas of image processing and analysis, mathematical modelling and computer graphics.

Dr John Yannis Goulermas graduated with a first class honours degree in computation from UMIST in 1994. He received the MSc by research and the PhD degrees in Electrical Engineering and Electronics at UMIST in 1996 and 2000, respectively. He worked in the Centre for Virtual Environments and the Centre for Rehabilitation and Human Performance Research of the University of Salford before joining the Department of Electrical Engineering and Electronics at the University of Liverpool as a Lecturer. His main research interests include pattern recognition, data analysis, artificial intelligence, machine vision and optimisation.

Dr Xiao-Jun Zeng Dr Zeng joined UMIST in October 2002. Before that, he was with Knowledge Support Systems Ltd (KSS) from February 1996 to September 2002 where he was a scientific developer, a senior scientific developer and the head of research. In KSS, he had involved in the research and development of several intelligent pricing decision support systems. He is a reviewer for IEEE Transaction on Fuzzy Systems, IEEE Transaction on Systems, Man and Cybernetics, International Journal of Intelligent and Fuzzy Systems and IFAC Automatica etc. He has published more than thirty papers in academic journals and conferences.

Dr Efstathios Milonidis received his first degree in Electrical Engineering from the National Technical University of Athens, his MSc in Control Engineering and his MPhil in Aerodynamics and Flight Mechanics from Cranfield Institute of Technology, and his PhD in Control Theory and Design from City University. He is currently a Lecturer in Control Engineering at the School of Engineering and Mathematical Sciences at City University. His main research interests are Discrete Time Control, Modelling and Simulation of Dynamical Systems, Systems Theory and Graph Methods for Multivariable Control Systems.

Figure Legends

Figure 1: Image showing different methods of background adjustments. The region inside the red circle represents the spot mask and the other regions bounded by coloured lines represent regions used for local background calculation by different methods. Green: used in QuantArray; blue: used in ScanAlyze; and pink: used in Spot (Yang et al., 2000).

Figure 2: Microarray expression of *Streptomyces coelicolor*.

Figure 3: Overall system structure for the microarray image analysis tool.

Figure 4: Breakdown of the steps in the task of addressing in the microarray image analysis tool.

Figure 5: Image thresholded with a value (a) 100 (b) 300 (c) 600 (d) 900.

Figure 6: Noise removal using opening (a) Original image (b) Noise preserved (c) noise removed by using difference image.

Figure 7: Effect of noise filtering (a) Original image, (b) Result of opening transformation.

Figure 8: First-order derivative locates the peaks/valleys in the signal.

Figure 9: Clustering tree structure using the short distance linking method.

Figure 10: The four clusters indicating the four meta-arrays.

Figure 11: The non-uniform grid superimposed on the (a) original image, (b) opened binary image.

Figure 12: The non-uniform grid superimposed on the image.

Figure 13: Overview of spot segmentation process.

Figure 14: GHTG Circle Detection, different peak size thresholds (a) 2500 (b) 1100 (c) 900.

Figure 15: (a) Original LoG edge detected image (b) different colours indicate; red: foreground/pixel area, blue: background area, white: vignette surrounding the spot and grey: edges of the spot.

Figure 16: A testing image showing a meta-grid of 10x10 possible spots.

Figure 17: Grids on the ScanAlyse tool are shown as red circles overlaying the image. These are also used for segmenting the spot, however, (a) is smaller than (b) and some parts of the spot in (b) are not contributing to the spot intensity features.

Figure 18: Comparison of segmentation (a) using TIGR SpotFinder (red line shows the segmentation area) and (b) the tool developed (black line shows the segmentation area)

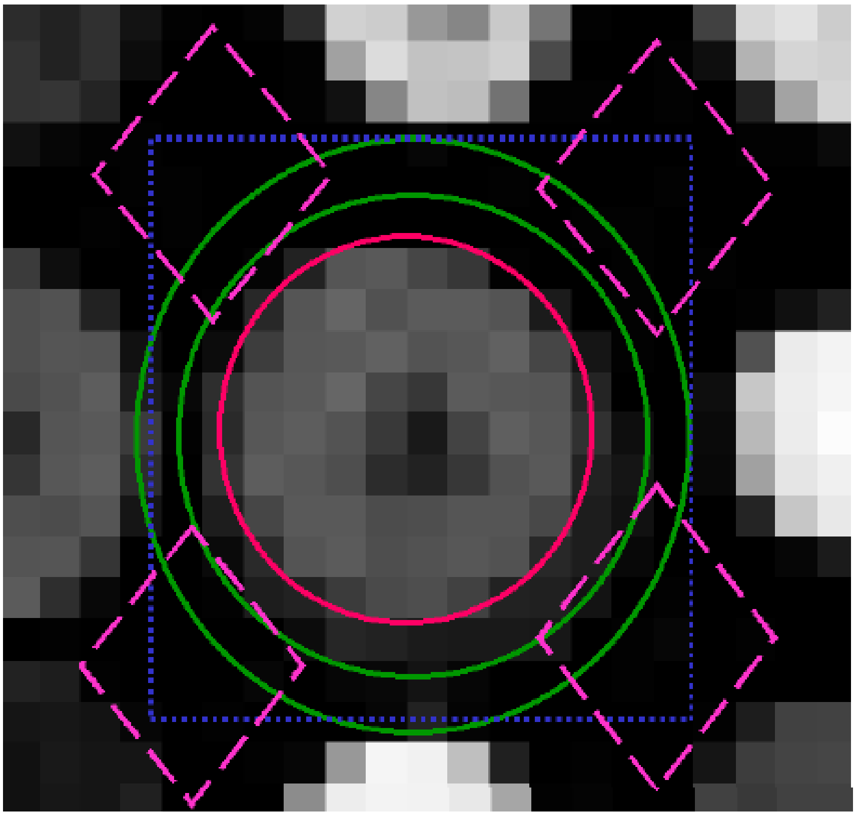

Figure 1

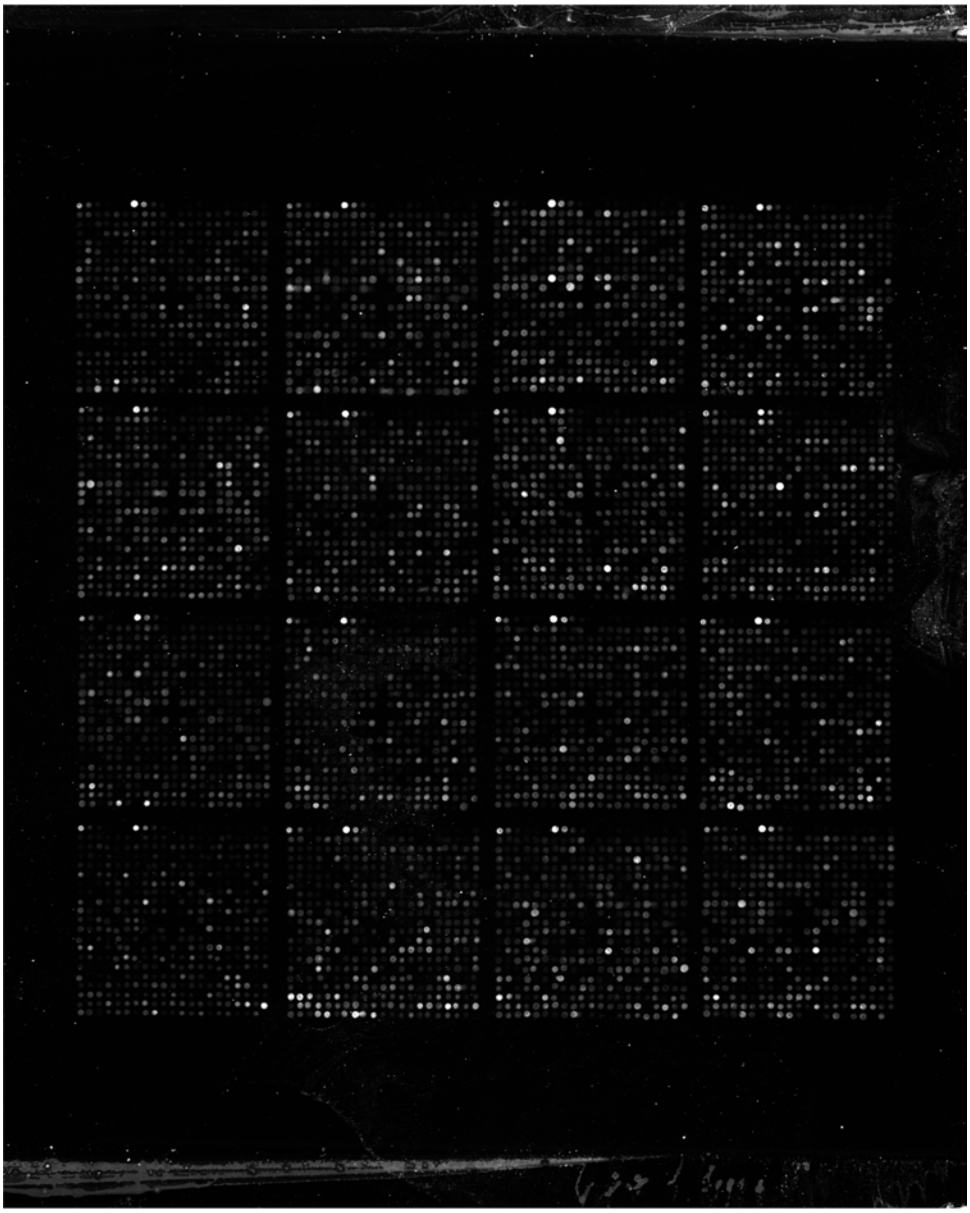

Figure 2

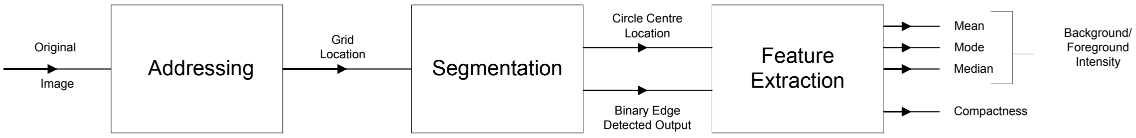
Original
Image
Addressing
Grid
Location
Segmentation
Circle Centre
Location
Binary Edge
Detected Output
Feature
Extraction
Mean
Mode
Median
Compactness
Background/
Foreground
Intensity

Figure 3

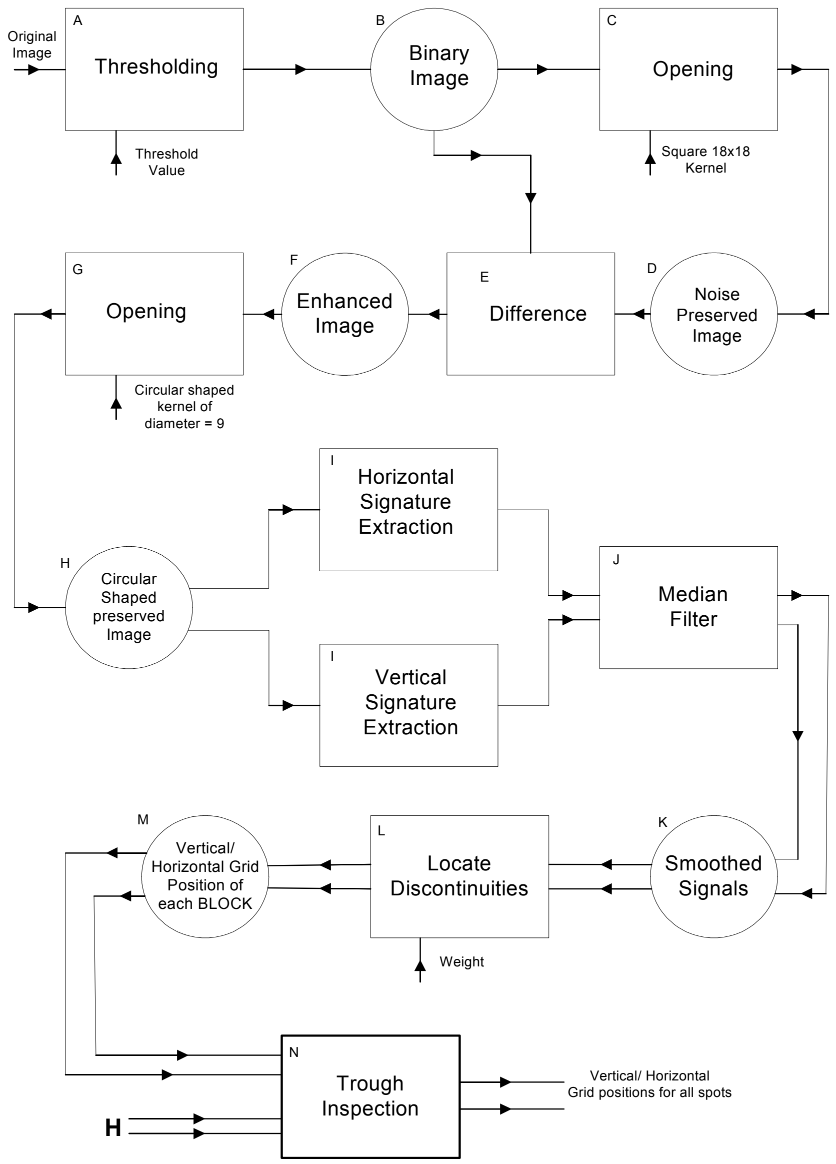

Original Image
A
Thresholding
Threshold Value
B
Binary Image
C
Opening
Square 18x18 Kernel
D
Noise Preserved Image
E
Difference
F
Enhanced Image
G
Opening
Circular shaped kernel of diameter = 9
H
Circular Shaped preserved Image
I
Horizontal Signature Extraction
I
Vertical Signature Extraction
J
Median Filter
K
Smoothed Signals
L
Locate Discontinuities
Weight
M
Vertical/ Horizontal Grid Position of each BLOCK
N
Trough Inspection
H
Vertical/ Horizontal Grid positions for all spots

Figure 4

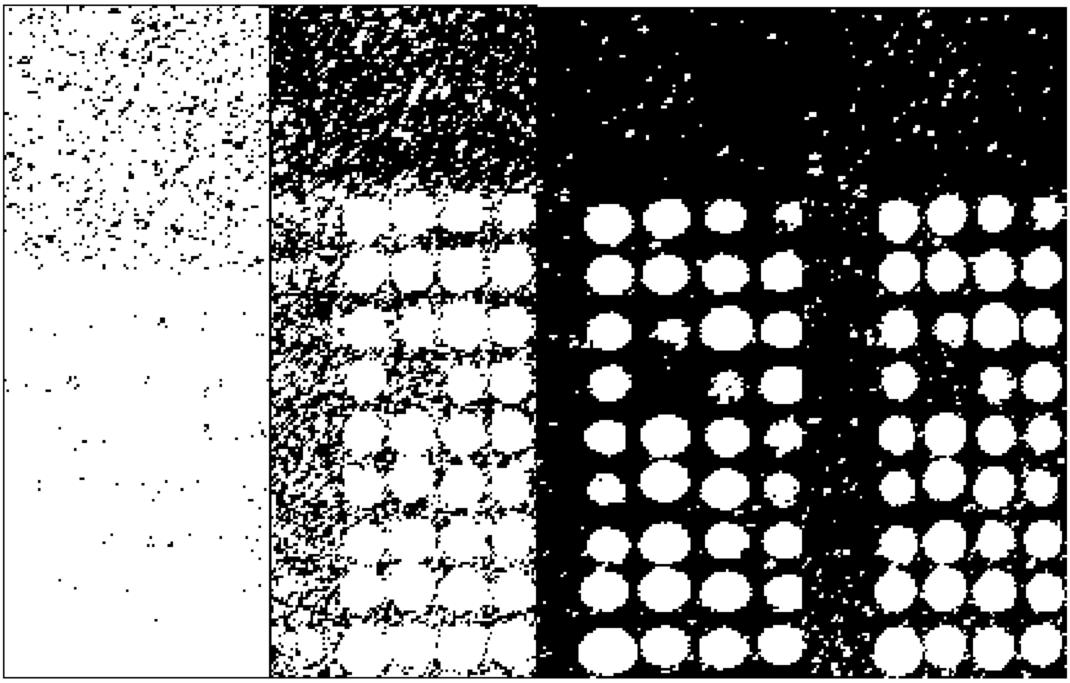

(a) (b) (c) (d)

Figure 5

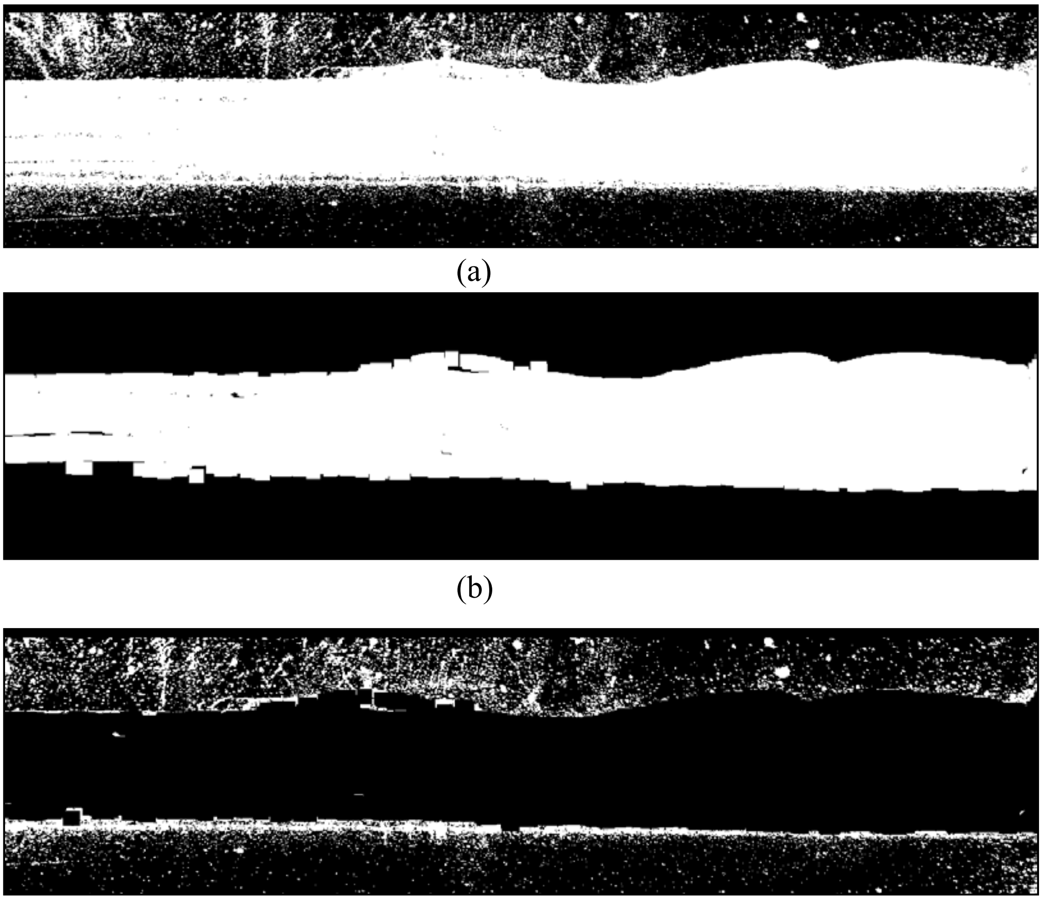

(a)

(b)

(c)

Figure 6

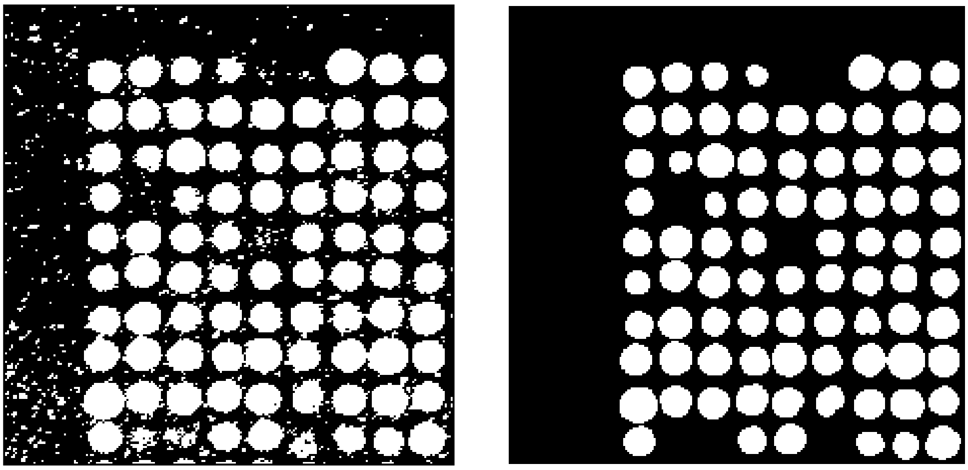

(a) (b)

Figure 7

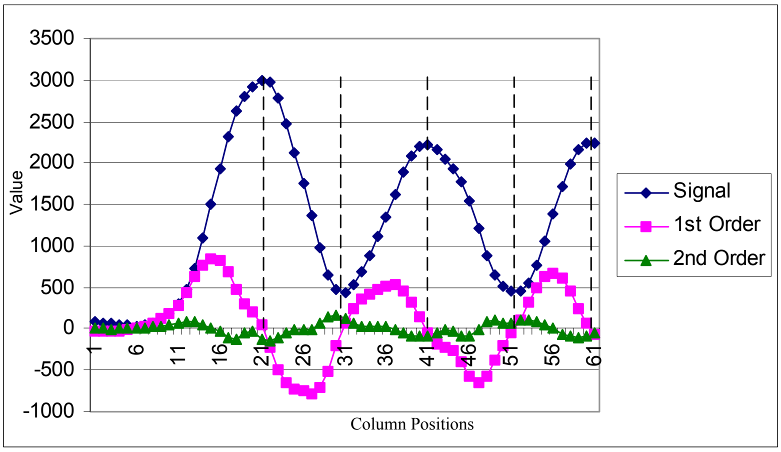
3500
3000
2500
2000
1500
1000
500
0
-500
-1000
Value
1
6
11
16
21
26
31
36
41
46
51
56
61
Column Positions
Signal
1st Order
2nd Order

Figure 8

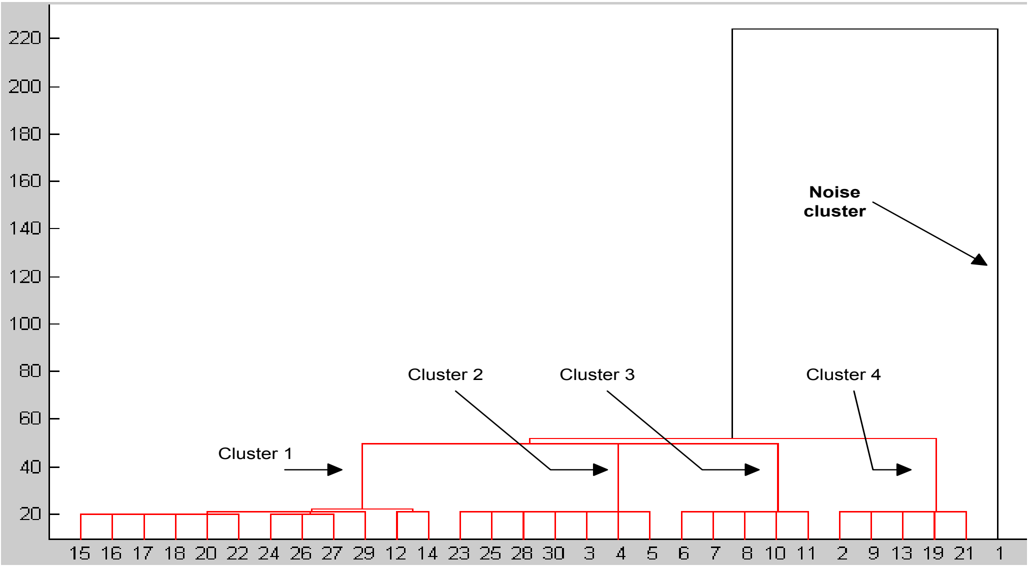

220
200
180
160
140
120
100
80
60
40
20
Noise cluster
Cluster 1
Cluster 2
Cluster 3
Cluster 4
15 16 17 18 20 22 24 26 27 29 12 14 23 25 28 30 3 4 5 6 7 8 10 11 2 9 13 19 21 1

Figure 9

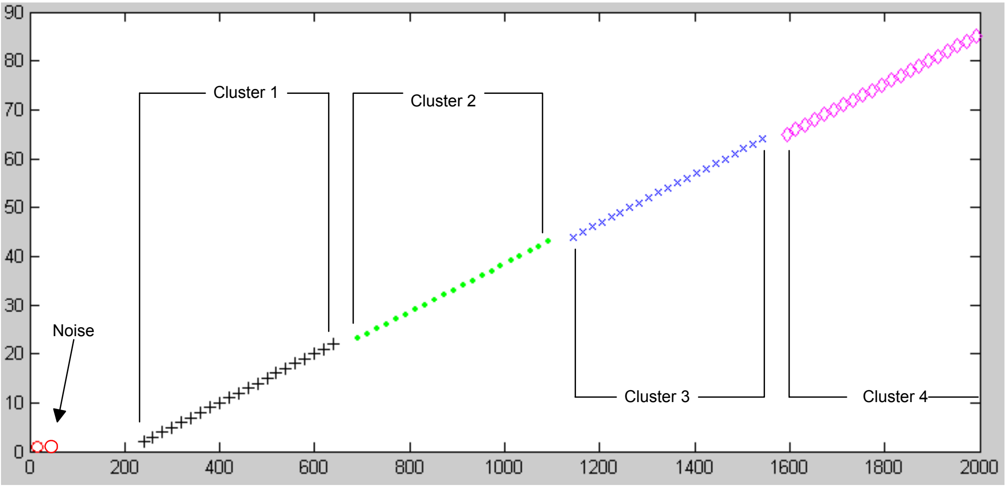
Cluster 1
Cluster 2
Cluster 3
Cluster 4
Noise
0
10
20
30
40
50
60
70
80
90
0
200
400
600
800
1000
1200
1400
1600
1800
2000

Figure 10

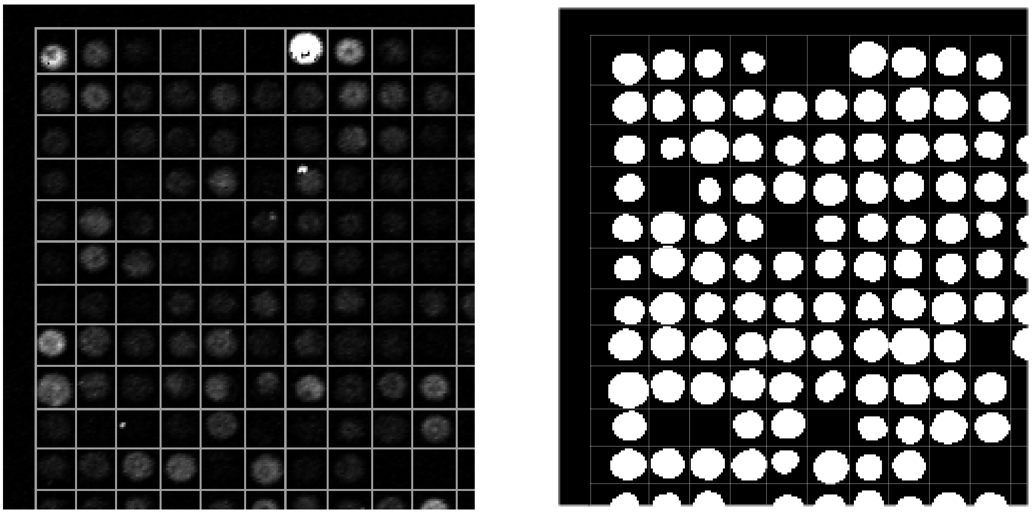

(a) (b)

Figure 11

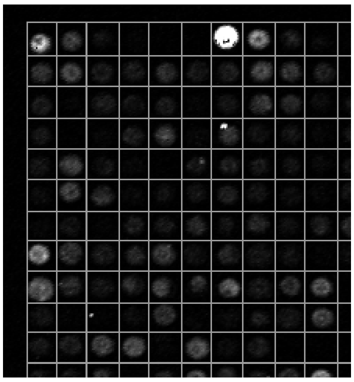

Figure 12

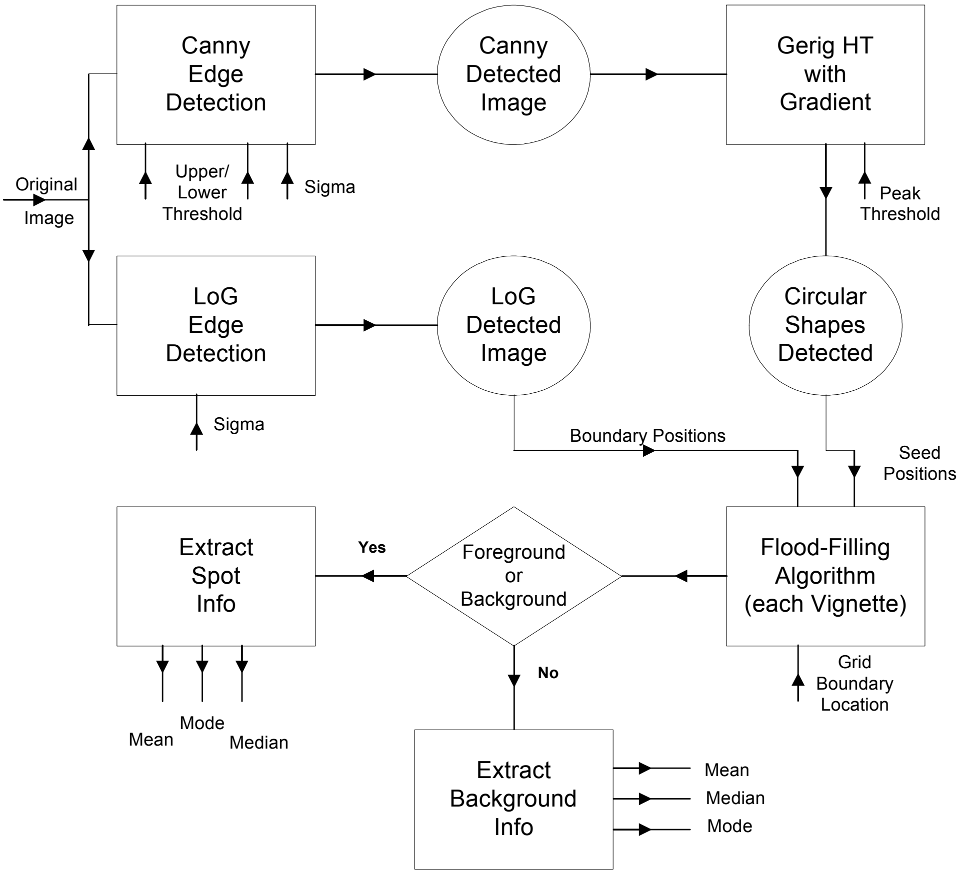
Canny Edge Detection
Canny Detected Image
Gerig HT with Gradient
Original Image
Upper/ Lower Threshold
Sigma
Peak Threshold
LoG Edge Detection
LoG Detected Image
Circular Shapes Detected
Sigma
Boundary Positions
Seed Positions
Extract Spot Info
Yes
Foreground or Background
Flood-Filling Algorithm (each Vignette)
No
Grid Boundary Location
Mode
Mean
Median
Extract Background Info
Mean
Median
Mode

Figure 13

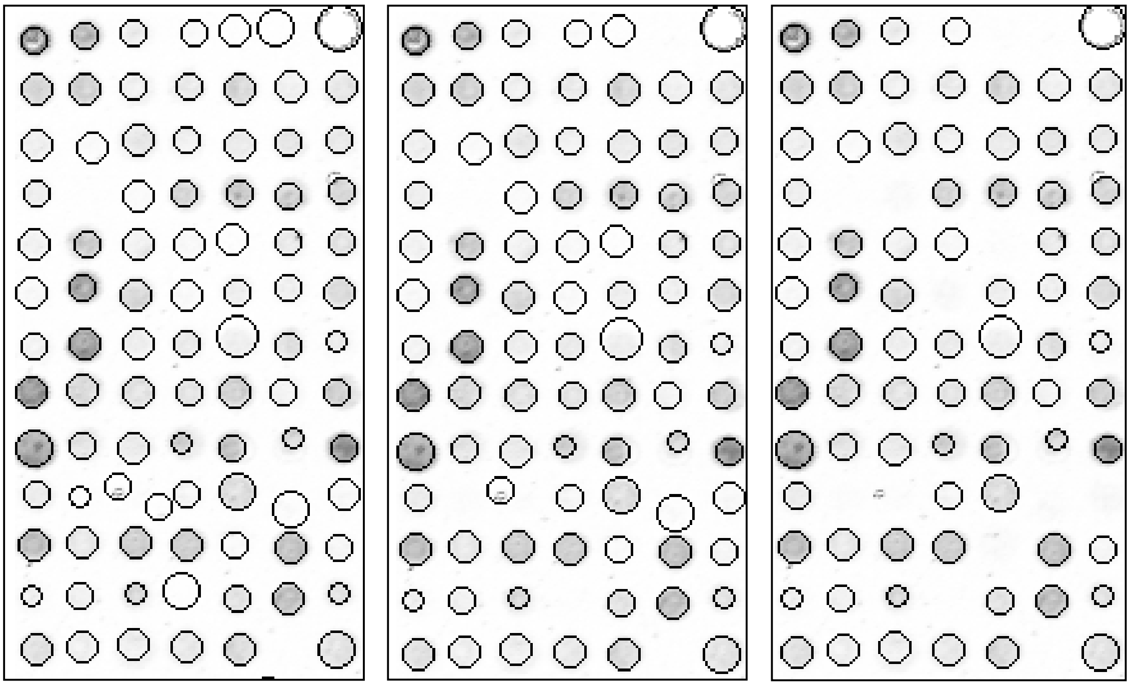

(a)

(b) (c)

Figure 14

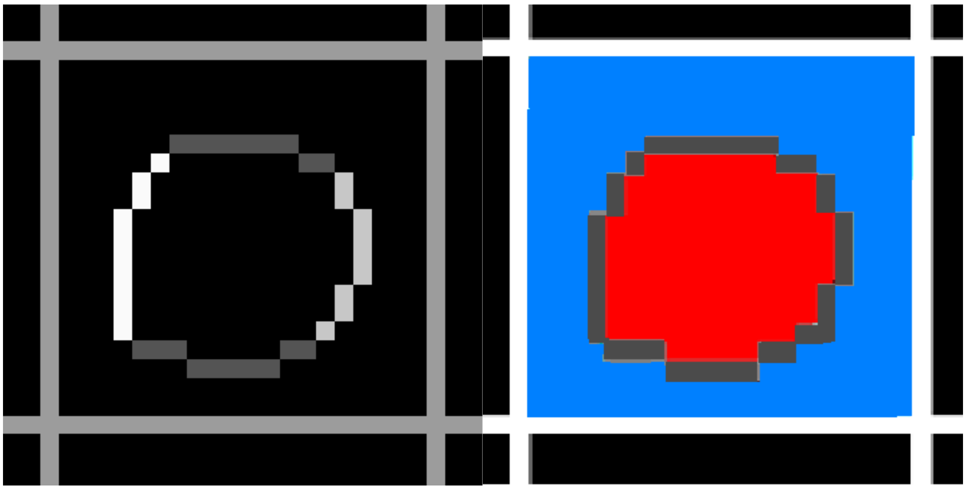

(a) (b)

Figure 15

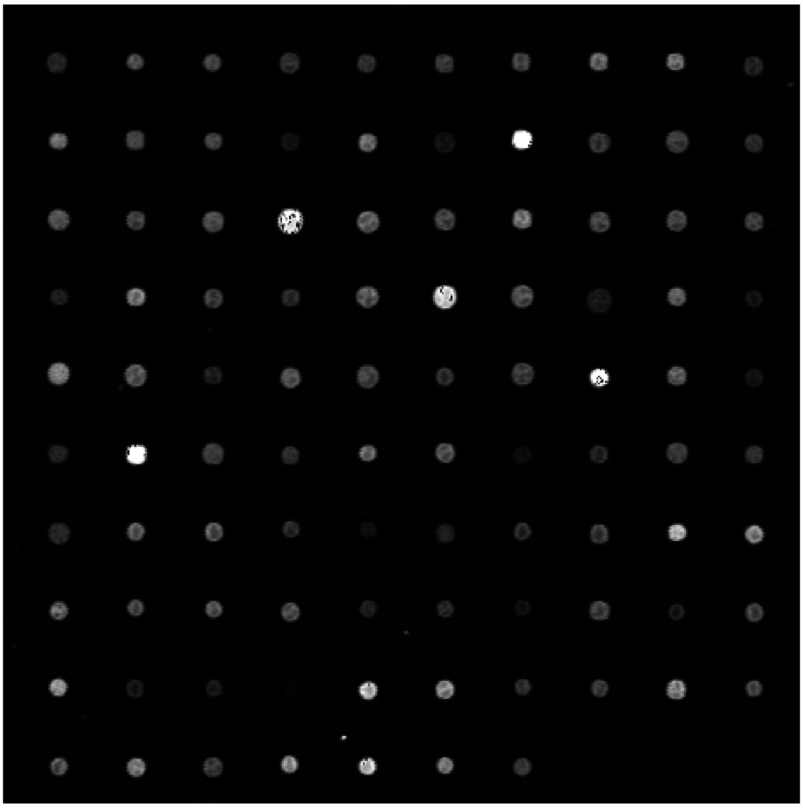

Figure 16

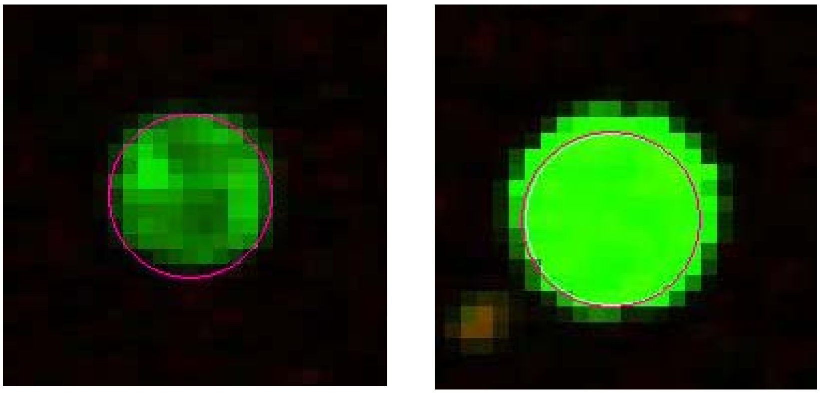

(a) (b)

Figure 17

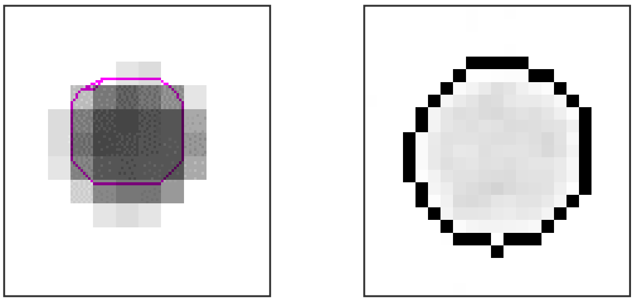

(a) (b)

Figure 18